TELKOMNIKA, Vol.17, No.6, December 2019, pp.3027~3043
ISSN: 1693-6930, accredited First Grade by Kemenristekdikti, Decree No: 21/E/KPT/2018
DOI: 10.12928/TELKOMNIKA.v17i6.13176

Hierarchical robust fuzzy sliding mode control for a class of simo under-actuated systems with mismatched uncertainties

Duc Ha Vu*[1], Shoudao Huang[2], Thi Diep Tran[3]
[1,2,3]College of Electrical and Information Engineering, Hunan University, Hunan, P.R. China
[1,3]Faculty of Electrical Engineering, Saodo University, Haiduong, Vietnam
*Correspondence: e-mail: vuhadhsd@hnu.edu.cn[1]

Abstract

The development of the algorithms for single input multi output (SIMO) under-actuated systems with mismatched uncertainties is important. Hierarchical sliding-mode controller (HSMC) has been successfully employed to control SIMO under-actuated systems with mismatched uncertainties in a hierarchical manner with the use of sliding mode control. However, in such a control scheme, the chattering phenomenon is its main disadvantage. To overcome the above disadvantage, in this paper, a new compound control scheme is proposed for SIMO under-actuated based on HSMC and fuzzy logic control (FLC). By using the HSMC approach, a sliding control law is derived so as to guarantee the stability and robustness under various environments. The FLC as the second controller completely removes the chattering signal caused by the sign function in the sliding control law. The results are verified through theoretical proof and simulation software of MATLAB through two systems Pendubot and series double inverted pendulum.

Keywords*: chattering phenomenon, fuzzy logic control, hierarchical robust fuzzy sliding mode control, single input multi output systems, under-actuated systems*

1. Introduction

Under-actuated systems are characterized by the fact that they have fewer actuators than the degree of freedom controlled [1]. Under-actuated systems are widely applied in practice as mentioned in [1, 2], free space flight robot, underwater robot, walking robot, mobile robot, Robot has flexible link, ships, helicopters etc. The studies of under-actuated mechanical systems are valuable in many applications. For example, if the under-actuated control system works well, the number of actuators can be reduced to make the system weight or system more compact. Advantages of studying under-actuated mechanical systems can also be found with walking robot, planes, spacecraft, etc. Sometimes, control algorithms for under-actuated systems can be used to restore partially broken system functions using the appropriate under-actuated control algorithm described in [3, 4]. The broken robot arm can still restore a functional part. Therefore, the development of control algorithms for under-actuated systems is very important. Their mathematical equations often include high nonlinear components and joints making their control designs difficult [5]. More recently, there has been a growing interest in under-actuated control systems in both theory and practice.

In this study, we focused on a class of SIMO under-actuated systems. This class is quite large, consisting of rotating or parallel inverted pendulum sub-systems, pendubot, TORA, etc. These systems are used not only to study control methods, but also as a teaching tool in university on the world. There are many control methods given such as energy-based control, passive-based control, hybrid control, intelligent control, etc was described in the documents [6-19]. Most articles only suggest control laws for a particular system. In fact, a general state space expression may describe this series of this systems. Therefore, it is possible to design a general control rule too for this series of systems rather than a control rule for a particular system.

The under-actuated SIMO system has uncertainty including matched and mismatched. Sliding mode control methods (SMC) can prevent matched uncertainty in the state of sliding

Received May 20, 2019; Revised June 30, 2019; Accepted July 18, 2019

mode. Regarding the control of SIMO under-actuated system, the mismatched uncertainty becomes more challenging. This paper focuses on dealing with mismatched uncertainties and chattering signals based on a fuzzy sliding mode controller for a class of SIMO under-actuated systems. In the past few years the sliding mode controller (SMC) has been widely used for control design of under-actuated nonlinear systems. SMC is an effective approach with maintaining stability and performance of control systems with accurate model [20-27]. The main advantage of SMC is that the external perturbations of the under-actuated system are handled by invariant characteristics with the sliding conditions of the system. However, the basic problem still exists in controlling complex systems using sliding controllers. For example, chattering phenomenon and mismatched uncertainties is one of its disadvantages. This approach has further research about fuzzy controller designs associated with sliding controller called fuzzy sliding mode controller (FSMC) [28–35]. Controller that is a combination of fuzzy logic control (FLC) and SMC provides a simple method to design the system. This method still maintains SMC positive qualities but reduce chattering phenomenon. The main advantage of FSMC is the dramatic reduction in chattering in the system. However, in controller [20-24] the parameters of the controller are not calculated to specific limits, in controller [25] the mismatched uncertainties are not handling, in controller [26] the ability to remove chattering signals is not mentioned. Controllers in [28-33] can't be applied to SIMO under-actuated systems with n subsystems and have not explicitly demonstrated the ability to remove chattering signals.

To overcome these disadvantages, in this paper author study the hierarchical robust fuzzy sliding mode controller (HRFSMC) for a variety of SIMO under-actuated systems with mismatched uncertainties. This controller applies to n subsystems, parameters are limited specifically and chattering signal elimination capabilities are demonstrated by clear theories. The hierarchical robust sliding control (HRSMC) method is first introduced as explained in [25, 26]. Then the author describes the procedure of designing the hierarchical robust fuzzy sliding mode controller (HRFSMC) for SIMO under-actuated systems with mismatched uncertainties. The simulation results show that the proposed controllers operate well. The paper presents the results and suggests that hierarchical robust fuzzy sliding mode controller have better performance than hierarchical robust sliding mode controllers.

2. The Hierarchical Robust Sliding Mode Controller (HRSMC)

Consider the state space expression of a series under-actuated SIMO systems with mismatched uncertainties include subsystems the following normal form:

$$\begin{cases} \dot{x}_1 = x_2 \\ \dot{x}_2 = f_1 + b_1 u + d_1 \\ \dot{x}_3 = x_4 \\ x_4 = f_2 + b_2 u + d_2 \\ \vdots \\ \dot{x}_{2n-1} = x_{2n} \\ \dot{x}_{2n} = f_n + b_n u + d_n \end{cases} \quad (1)$$

therein $X = [x_1, x_2, \ldots, x_{2n}]^T$ is state variable vector; f_i and $b_i\,(i = 1,2,\ldots,n)$ are nonlinear functions of the state vector; u is the input control signal. In (1) can represent classes of systems with n, f_i and b_i is different, d_i is mismatched uncertainties, include system uncertainties and external disturbances, and d_i is limited by $|d_i| \le \bar{d}_i$ where $\bar{d}_i$ is a known positive constant; If $n = 2$, (1) can represent Pendubot, the cart single inverted pendulum system. If $n = 3$ represent for cart double inverted pendulum system; if $n = 4$, it could be considered a cart triple inverted pendulum system and so on, based on the physical structure, the series of under-actuated systems can be divided into multiple subsystems. For example, a triple inverted pendulum system can be divided into four sub-systems: the upper pendulum, the middle pendulum, the lower pendulum, and cart. The such system in (1) created from n subsystems. The ith subsystem consists of its state variables and state space expressions as follows:

$$\begin{cases} \dot{x}_{2i-1} = x_{2i} \\ \dot{x}_{2i} = f_i + b_i u \end{cases} \quad (2)$$

According to [25] the design of hierarchical sliding control (HSMC) is shown in Figure 1. The sliding surface of the ith subsystem is defined as follows:

$$s_i = c_i x_{2i-1} + x_{2i} \tag{3}$$

with c_i is positive constant and limit of c_i as presented in [25] is $0 < c_i < c_{i0}$

$$\text{with } c_{i0} = \left|\lim_{X\to 0}(f_i/x_{2i})\right| \tag{4}$$

derivative s_i follow t time in (3) we have:

$$\dot{s}_i = c_i \dot{x}_{2i-1} + \dot{x}_{2i} = c_i x_{2i} + f_i + b_i u \tag{5}$$

get $\dot{s}_i = 0$in (5) the control voltage of the ith subsystem is as follows:

$$u_{eqi} = -(c_i x_{2i} + f_i)/b_i \tag{6}$$

according to Figure 1, the I th sliding class is determined:

$$S_i = \lambda_{i-1} S_{i-1} + s_i \tag{7}$$

there in $\lambda_{i-1}(\mathrm{i} = 1, 2, \ldots \mathrm{n})$ is constant and $\lambda_0 = S_0 = 0$. Take $i = n$ according to [25, 26] hierarchical robust sliding control law as follows:

$$u = u_n + u_{cn} = \frac{\sum_{r=1}^{n}(\prod_{j=r}^{n} a_j) b_r u_{eqr}}{\sum_{r=1}^{n}(\prod_{j=r}^{n} a_j) b_r} - \frac{k_n S_n + \eta_n \, sgn\, S_n}{\sum_{r=1}^{n}(\prod_{j=r}^{n} a_j)\, b_r} + \frac{\sum_{r=1}^{n}(\prod_{j=r}^{n} a_j)\bar{d}_r}{\sum_{r=1}^{n}(\prod_{j=r}^{n} a_j) b_r} \tag{8}$$

from (7) and (8) we have a hierarchical slider control structure schematic shown in Figure 2.

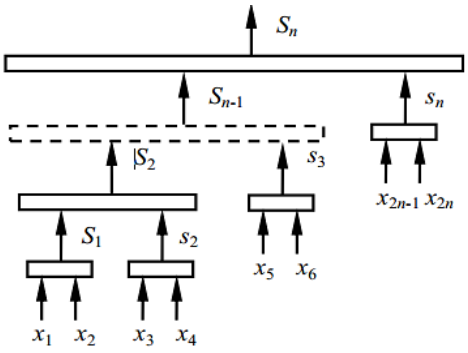

Figure 1. Hierarchical structure of the sliding surfaces

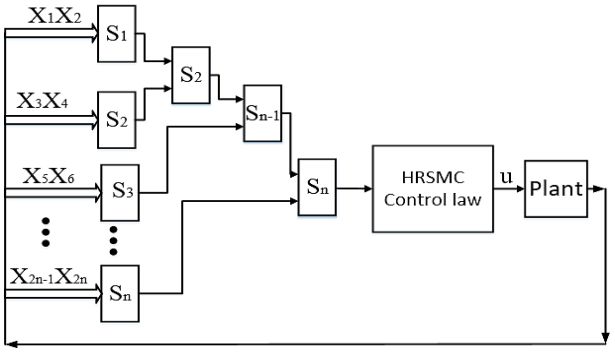

Figure 2. Architecture schematic of HRSMC control system

3. The Hierarchical Robust Fuzzy Sliding Mode Controller (HRFSMC)

The design of the hierarchical robust fuzzy sliding mode controller (HRFSMC) for a series of under-actuated systems with mismatched uncertainties is derived from the following idea. In control rule of the under-actuated system represented by (8) with $\mathrm{sgn}\, S_n$ function, this is the main cause of chattering in the system. A method of removing the chattering signal is to replace the fixed parameter in (8) by a variable value through the fuzzy controller. Value η_n will change under the extent of sliding surface.When S_n is extremely small, namely the state variables move closer to zero then η_n will also decrease to zero to make the $\mathrm{sgn}\, S_n$ function no longer affect the u_n control signal. We have:

$$\lim_{\eta_n \to 0} \eta_n \, sgn\, S_n = 0 \tag{9}$$

However, if η_n is small from the beginning, the uncontrolled signal will move very slowly towards the equilibrium position. But if η_n from the beginning is extremely large, the state variables of the system will quickly advance to the equilibrium position, but at equilibrium position, the system will fluctuate greatly. Therefore, the value η_n initial should be large enough so that u_n can pull the system to equilibrium position. When the system is in equilibrium then the smaller η_n is the better it is. To implement the above idea, the author changes the value of η_n based on value of sliding surface S_n. We will compute η_n through a fuzzy controller, the input of the fuzzy controller is the value of the S_n sliding surface. The structure of hierarchical robust fuzzy sliding mode controller (HFSMC) is shown in Figure 3. The fuzzy rules in the "Fuzzy logic controller" block are shown in Table 1.

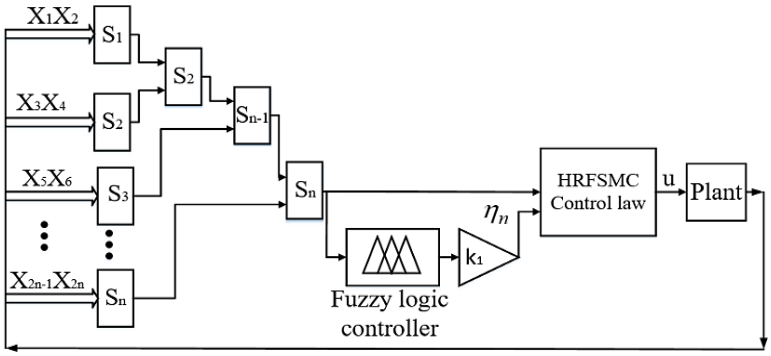

Figure 3. Architecture schematic of the HRFSMC controller for under-actuated systemsv

Table 1. Rule in the Fuzzy Block

The number of fuzzy rules	S_n	η_n
1	A	A
2	B	B
3	C	C
4	D	D
5	E	E
6	F	F
7	G	G

The membership functions of linguistic labels A, B, C, D, E, F, G for the term S_n are shown in Figure 4. The membership functions of linguistic labels A, B, C, D, E, F, G for the term η_n are shown in Figure 5. The membership function in Figure 4 and Figure 5 is norm form. To modify the parameters of the fuzzy controller, selecting the value of the post-processing block k_1 shown in Figure 3 is necessary. The k_1 parameter determines the ability to disappear the chattering signal in the system. The choice of the k_1 parameter can be performed by a search algorithm, such as a genetic algorithm or herd algorithm, or a simple false test.

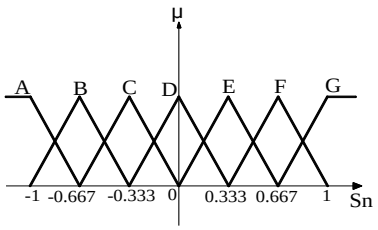

Figure 4. Membership function of each input

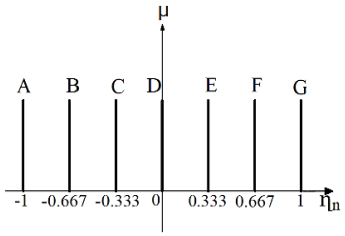

Figure 5. Membership function of each output

4. Denonstrate Stability and Capability of Eliminating Chattering Signal of Hierarchical Robust Fuzzy Sliding Mode Controller (HRFSMC)

Two theorems will be proved in this section. Theorem 1 is to analyze the asymptotic

stability of all sliding layers. Theorem 2 involves analyzing the ability of eliminating chattering signal of the HFSMC controller. Theorem 1: consider the classes of the under-actuated system (1). If the control rule is chosen as (8) and the i[th] layer of sliding surface is defined as (7) $(i = n)$, then the asymptotic stability. Proof: The Lyapunov function of i^{th} $(i = n)$ layer of sliding surface is selected:

$$\bar{V}_n = \bar{S}_n^2/2 \tag{10}$$

by considering the stability of the i^{th} layer $(i = n)$ of sliding surface, from [26] we take:

$$\dot{\bar{S}}_n = \left[\sum_{r=1}^{n}(\prod_{j=r}^{n} a_j)\,\bar{d}_r + \sum_{r=1}^{n}(\prod_{j=r}^{n} a_j)\,b_r u_{eqr}\right] - k_n S_n - \eta_n\, sgn\, S_n \tag{11}$$

differentiate $\bar{V}_n$ with respect to time t in (10), then from (11) we obtain:

$$\dot{\bar{V}}_n = \bar{S}_n.\dot{\bar{S}}_n = S_n\left[\sum_{r=1}^{n}(\prod_{j=r}^{n} a_j)\,d_r\right] - |S_n|\left|\sum_{r=1}^{n}(\prod_{j=r}^{n} a_j)\,\bar{d}_r\right| - \eta_n|S_n| - k_n S_n^2 \tag{12}$$

let integrate the two sides of (12) we obtain:

$$\int_0^t \dot{\bar{V}}_n\, d\tau = \int_0^t\left[S_n\left[\sum_{r=1}^{n}(\prod_{j=r}^{n} a_j)\,d_r\right] - |S_n|\left|\sum_{r=1}^{n}(\prod_{j=r}^{n} a_j)\,\bar{d}_r\right| - \eta_n|S_n| - k_n S_n^2\right] d\tau \tag{13}$$

with

$$\bar{V}_n(0) = \bar{V}_n(t) + \int_0^t\left[S_n\left[\sum_{r=1}^{n}(\prod_{j=r}^{n} a_j)\,d_r\right] - |S_n|\left|\sum_{r=1}^{n}(\prod_{j=r}^{n} a_j)\,\bar{d}_r\right| - \eta_n|S_n| - k_n S_n^2\right] d\tau$$
$$\geq \int_0^t(\eta_n|S_n| + k_n S_n^2)\, d\tau \tag{14}$$

hences

$$\lim_{t\to\infty}\int_0^t(\eta_n|S_n| + k_n S_n^2)\, d\tau \leq \bar{V}_n(0) < \infty \tag{15}$$

the barbalat lemma exists

$$\lim_{t\to\infty}(\eta_n|S_n| + k_n S_n^2) d\tau \leq \bar{V}_n(0) < \infty \tag{16}$$

from (16), it means that $\lim_{t\to\infty} S_n = 0$then the n^{th}layer of sliding surface is asymptotically stable.

Theorem 2: Consider a variety of under-actuated systems (1), If the control rule is defined as (8) and the fixed parameter η_n in (8) is substitute by a replacement cost based on the magnitude of S_n sliding surface through the fuzzy controller, the chattering signal in the system will be completely eliminated.

Proof: From (8), it is clear that the main component causing the chattering phenomenon in the system is the function $\eta_n\, sgn\, S_n$. To overcome this phenomenon, we add a fuzzy processing element in the Controller to eliminate the $sign$. The sliding surface S_n is fuzzy as shown in Figure. 4. The fuzzy rule system is shown in Table 1 as follows:

R^1 : If S_n is A Then η_n^1 = A
R^2 : If S_n is B Then η_n^2 = B
R^3 : If S_n is C Then η_n^3 = C
R^4 : If S_n is D Then η_n^4 = D
R^5 : If S_n is E Then η_n^5 = E
R^6 : If S_n is F Then η_n^6 = F
R^7 : If S_n is G Then η_n^7 = G

by the focal defuzzification method parameter η_n is defined:

$$\eta_n = \frac{\sum_{i=1}^{7}\beta_i\eta_n^i}{\sum_{i=1}^{7}\beta_i} \tag{17}$$

in there β_i is the correctness of the i^{th}rule:

$$\begin{aligned}\beta_1 &= \mu_A(S_n)\\ \beta_2 &= \mu_B(S_n)\\ \beta_3 &= \mu_C(S_n)\\ \beta_4 &= \mu_D(S_n)\\ \beta_5 &= \mu_E(S_n)\\ \beta_6 &= \mu_F(S_n)\\ \beta_7 &= \mu_G(S_n)\end{aligned} \tag{18}$$

from (17) and (18) we obtain:

$$\lim_{S_n\to 0}\eta_n = \lim_{S_n\to 0}\frac{\sum_{i=1}^{7}\beta_i\eta_n^i}{\sum_{i=1}^{7}\beta_i} = 0 \tag{19}$$

from (19) deduce

$$\lim_{S_n\to 0}\eta_n\, sgn\, S_n = 0 \tag{20}$$

according to theorem 1 we have:

$$\lim_{t\to\infty} S_n = 0 \tag{21}$$

from (20) and (21) we deduce:

$$\lim_{t\to\infty}\eta_n\, sgn\, S_n = 0 \tag{22}$$

according to (22) when time t tends to ∞, function $\eta_n \operatorname{sgn} S_n$ is completely eliminated in control rule (8). Thus, chattering signal at the equilibrium position has been completely eliminated in the hierarchical robust fuzzy sliding controller (HFSMC).

5. Simulation Result

The Pendubot and cart double inverted pendulum systems are two typical under-actuated systems, usually used to verify the feasibility of new control methods. Their mathematical equations have the same expressions as (1) with different f_i, b_i, and n, d_i is mismatched uncertainties, include system uncertainties and external disturbances, and d_i is limited by $|d_i| \le \bar{d}_i$ where $\bar{d}_i$ is a known positive constant. In this section, the control method presented will be applied to enhance the control of the Pendubot system and the cart double inverted pendulum system. The simulation results show that this control method is feasible.

5.1. Pendubot

The pendubot system shown in Figure 6 is made up of two subsystems: Link 1 (notation number 1) with one actuator and link 2 (notation number 2) without actuator. Its control objective is to control link 1, link 2 balance and stability at the desired position. The symbols in Figure 6 are defined as follows: $\boldsymbol{\theta_1}$ is the angle of link 1 to the horizontal line, θ_2 is the angle of link 2 for link 1. m_i, l_i and l_{ci} is the mass, length and distance to the center of link i. Here $i = 1,2$; τ_1 is the control moment. Taking $n = 2$ in (1) the state space equation of the pendubot system is as follows:

$$\begin{cases}\dot{x}_1 = x_2\\ \dot{x}_2 = f_1 + b_1 u + d_1\\ x_3 = x_4\\ \dot{x}_4 = f_2 + b_2 u + d_2\end{cases} \tag{23}$$

Here $x_1 = \theta_1 - \pi/2$ is the angle of the link 1 for the vertical line, $x_3 = \theta_2$ is the angle of the link 2 for link 1; x_4 is the angular velocity of link 2. $u = \tau_1$ is the input control signal. Expressions f_1, f_2, b_1 and b_2 are shown in [24], d_1 and d_2 are the mismatched uncertain term with known bound called $\bar{d}_1$ and $\bar{d}_2$. Both components of the mismatched uncertain d_1 and d_2

are set to $0.1 \times [2 \times \text{rand}()\text{-}1]$. where rand() is Matlab command to generate a random number in the range (0,1). So, the bounds of the mismatched uncertain tems $\bar{d}_1$ and $\bar{d}_2$ can be defined as 0.2. In comparison between the HRSMC controller and the HRFSMC controller, the parameters of the pendubot are chosen according to [24] and [9]:

$$q_1 = 0.0308\text{kg.m}^2, q_2 = 0.0106\text{kg.m}^2$$
$$q_3 = 0.0095\text{kg.m}^2, q_4 = 0.2086\text{kg.m}^2$$
$$q_5 = 0.0630\text{kg.m}^2, g = 9.81\text{m.s}^{-2}$$

according to (4), the boundary of c_1, c_2 is calculated as follows:

$$\begin{cases} c_{10} = g|(q_3 q_5 - q_2 q_4)/(q_1 q_2 - q_3^2)| = 66.97 \\ c_{20} = g|[q_5(q_1 + q_3) - q_4(q_2 + q_3)]/(q_1 q_2 - q_3^2)| = 68.68 \end{cases}$$

the HRSMC controller parameter of the $c_1 = 5.807, c_2 = 7.346, a_1 = 1.826, k_2 = 3.687$ and $\eta_2 = 1.427$. Initial state vector$\theta_0 = \left[\frac{\pi}{2} + 0.1, 0.1, -0.1, -0.2\right]^T$. The desired state vector is $\theta_d = [0,0,0,0]^T$.

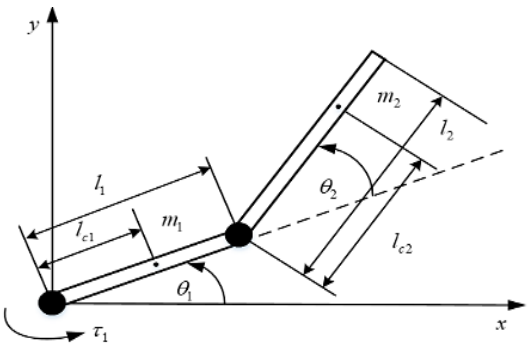

Figure 6. Structure of the pendubot system

The HRFSMC controller parameters of the pendubot system are selected the same as parameters of HRSMC controller. However, the HRFSMC controller has an additional parameter selected as $k_1 = 0.01$ and $k_1 = 5$. To see that the HRFSMC controller is more efficient than the HRSMC controller. We have simulated in 2 cases $k_1 = 0.01$ and $k_1 = 5$ of HRFSMC controller when compared with HRSMC controller. With smaller k_1 value, the ability to remove chattering signals of HRFSMC controller will be better than HRSMC controllers. But to achieve this capability, the system will respond more slowly, the transition value will be larger. In contrast to the larger k_1 value, HFSMC controller responds more quickly, larger transient value will have a larger chattering. To clarify this issue, let's look at the simulations below.

Figures 7, 8, 9, 10 compare simulation results of two controllers HRSMC and HRFSMC pendubot systems with $k_1 = 0.01$. It shows that angle of link1, link2 of HRSMC and HRFSMC controllers converge to the equilibrium position for about 0.6 and 1.5 seconds. The action torque on link 1 of the HRFSMC controller has an oscillation which is completely disappeared compared with action torque on link 1 of the HRSMC controller. The angles link 1 and link 2 of the HRFSMC controller has an oscillation which is completely disappeared compared with angles link 1 and link 2 of the HRSMC controller. However, the HRSMC controller responds faster than the HRFSMC controller with $k_1 = 0.01$.

Figures 11, 12, 13 compare simulation results of two controllers HRSMC and HRFSMC pendubot systems with $k_1 = 5$. It shows that angle of link1, link2 of HRSMC and HRFSMC controllers converge to the equilibrium position for about 0.6 seconds. The action torque on link 1 of the HRFSMC controller has an oscillation which is greater compared with action torque on link 1 of the HRSMC controller. The angles link 1 and link 2 of the HRFSMC controller has an oscillation which is greater compared with angles link 1 and link 2 of the HRSMC controller. However, the HRFSMC controller responds faster than the HRSMC controller with $k_1 = 5$.

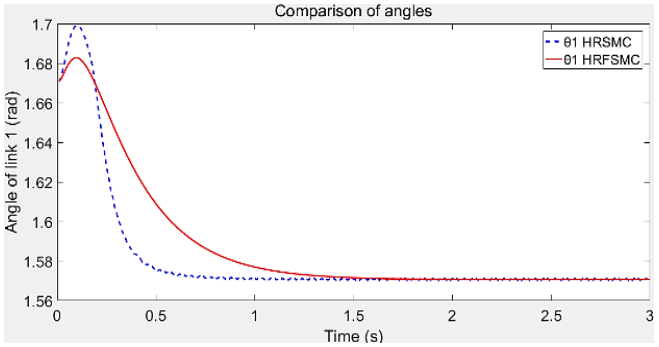

(a)

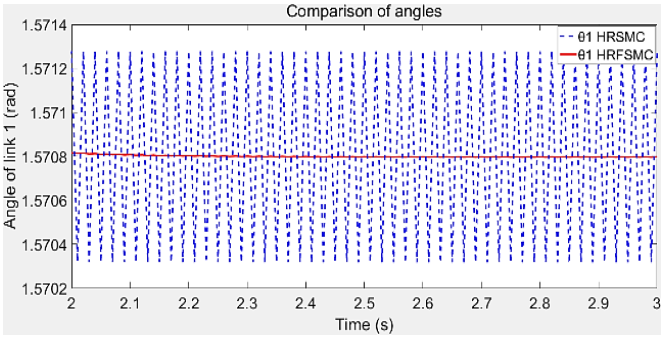

(b)

Figure 7. The angle link 1 of pendubot when using HRSMC controller and the HRFSMC controller with $k_1 = 0.01$ (a) θ_1 in time series format; (b) Zoomed-in time frame of θ_1 (2–3 s)

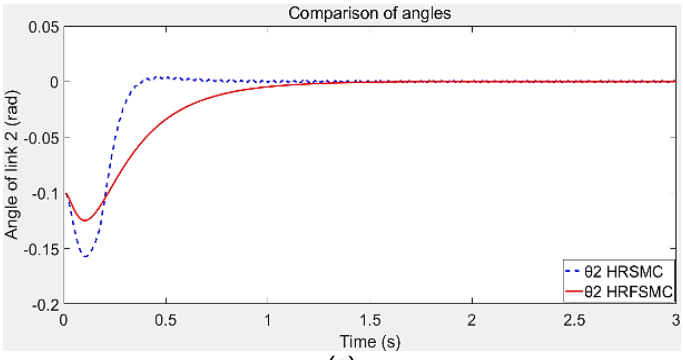

(a)

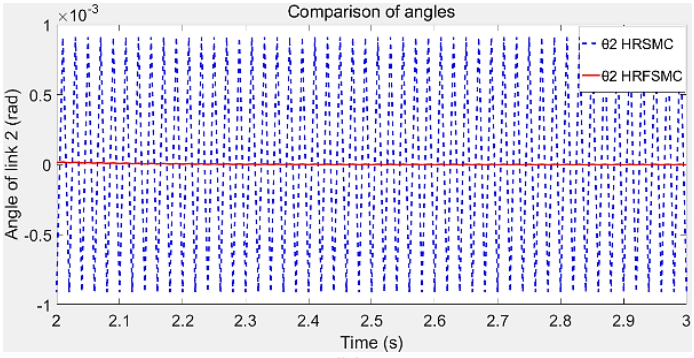

(b)

Figure 8. The angle link 2 of pendubot when using HRSMC controller and the HRFSMC controller with $k_1 = 0.01$ (a) θ_2 in time series format; (b) Zoomed-in time frame of θ_2 (2 – 3s)

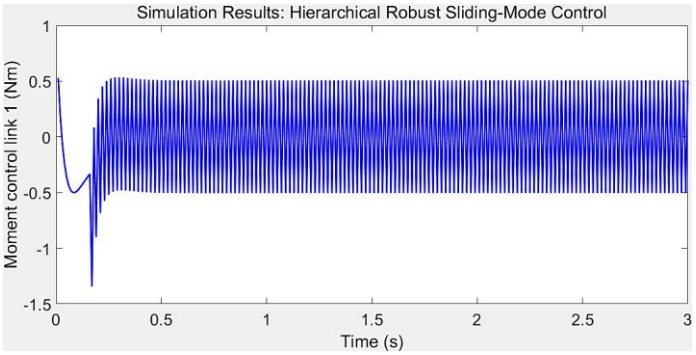

Figure 9. Action torque on link 1 of the pendubot when using the HRSMC controller

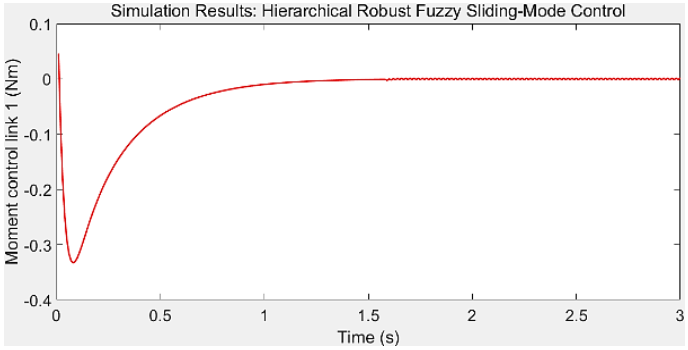

Figure 10. Action torque on link 1 of the pendubot using the HRFSMC controller with $k_1 = 0.01$

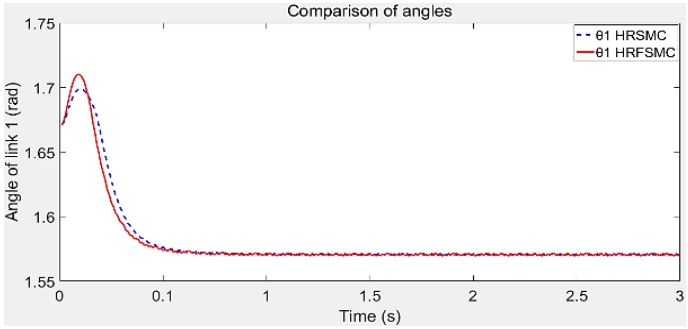

(a)

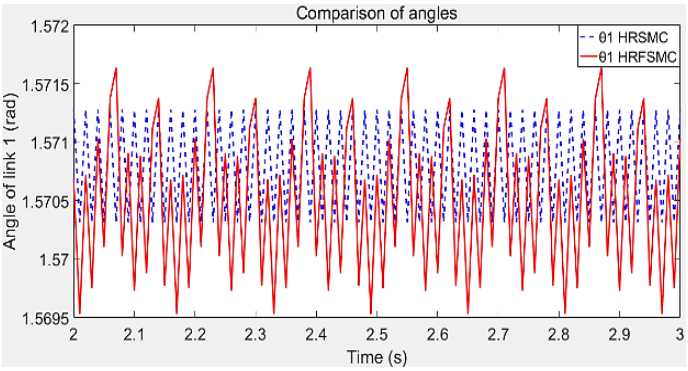

(b)

Figure 11. The angle link 1 of pendubot when using HRSMC controller and the HRFSMC controller with $k_1 = 5$ (a) θ_1 in time series format; (b) Zoomed-in time frame of θ_1 (2 – 3s)

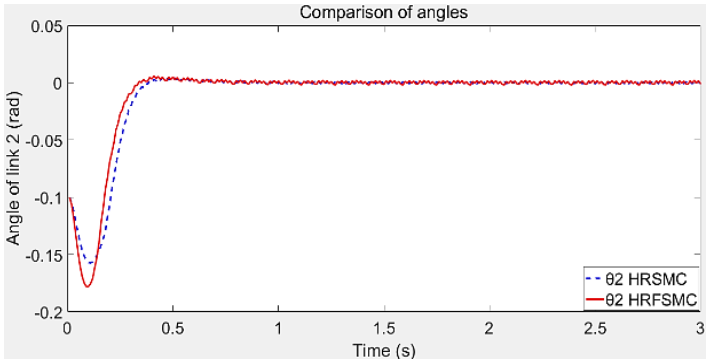

(a)

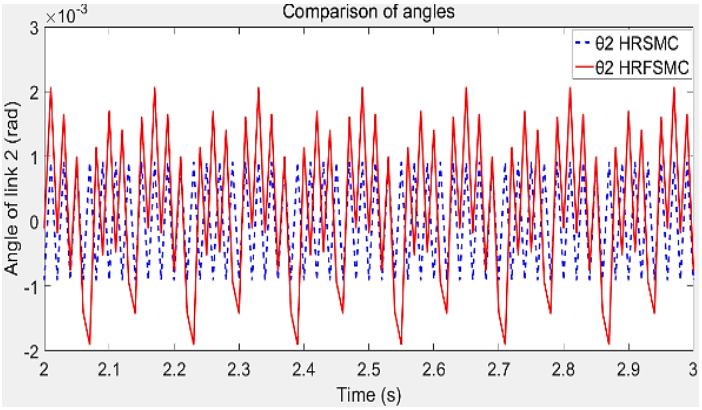

(b)

Figure 12. The angle link 2 of pendubot when using HRSMC controller and the HRFSMC controller with $k_1 = 5$ (a) θ_2 in time series format; (b) Zoomed-in time frame of θ_2 (2 – 3s)

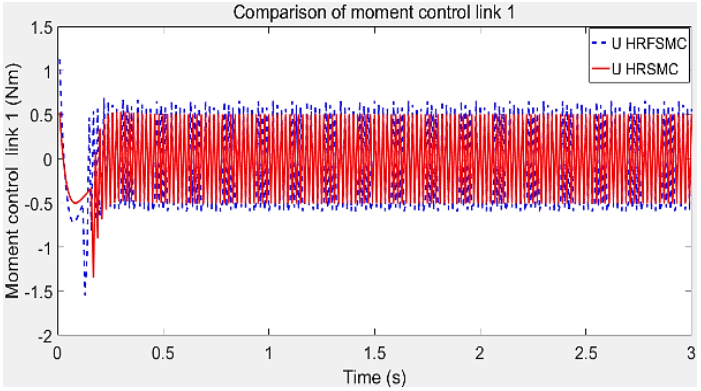

Figure 13. Action torque on link 1 of the pendubot when using the HRSMC controller and the HRFSMC controller with $k_1 = 5$

5.2. The Cart Double Inverted Pendulum System

The cart double inverted pendulum system is coupled by two pendulum in a moving cart as shown in Figure 14. The system consists of three subsystems: the upper pendulum, the under pendulum and cart. Its control objective is to keep stable to equilibrium two upright vertical pendulum and to bring the cart to its equilibrium position [22].

The symbols in Figure 14 are defined as follows: θ_1 is the angle of the inverted pendulum with vertical line. θ_2 is the angle of the inverted pemdulum with vertical line, which is the control force. Taking $n = 3$ in (1), the state-space expression of the cart inverted pendulum system is defined as follows:

$$\begin{cases} \dot{x}_1 = x_2 \\ \dot{x}_2 = f_1 + b_1 u + d_1 \\ \dot{x}_3 = x_4 \\ \dot{x}_4 = f_2 + b_2 u + d_2 \\ \dot{x}_5 = x_6 \\ \dot{x}_6 = f_3 + b_3 u + d_3 \end{cases} \quad (24)$$

Here $x_1 = \theta_1; x_3 = \theta_3; x_5 = x$; x_2 is angular velocity of under pendulum; x_4 is the angular velocity of the pendulum; x_6 is the angular velocity of the cart; u is the control signal, $f_i$and $b_i (i = 1,2,3))$ is defined in [31]. d_1, d_2 and d_3 are the mismatched uncertain term with known bound called $\bar{d}_1, \bar{d}_2$ and $\bar{d}_3$. Both components of the mismatched uncertain d_1, d_2 and d_3 are set to $0.1 \times [2 \times \text{rand}()\text{-}1]$. where rand () is Matlab command to generate a random number in the range (0,1). So, the bounds of the mismatched uncertain tems $\bar{d}_1, \bar{d}_2$ and $\bar{d}_3$ can be defined as 0.2.

In comparison between the HRSMC controller and the HRFSMC controller, the parameters of the cart double inverted pendulum are chosen according to [30]. Mass of cart $M = 1\,\text{kg}$ Mass of below pendulum $m_1 = 1\,\text{kg}$. Mass of above pendulum. The length of the above inverted pendulum $l_1 = 0.1\,m$. The length of the below inverted pendulum $l_2 = 0.1\,m$. The gravitational acceleration $g = 9.81\text{m.s}^{-2}$. According to (4) the boundary lines of c_1, c_2, c_3 are computed as follows:

$$\begin{cases} c_{10} = g \left| \frac{A^2(B/3 - m_2 l_2/4)}{(m_2/4 - A/3)(B^2 - AC) - m_2(B - Al_1)^2/4} \right| \\ = 294.39 \\ c_{20} = g \left| \frac{A^2(C - Bl_1)/2}{l_2[(m_2/4 - A/3)(B^2 - AC) - m_2(B - Al_1)^2/4]} \right| \\ = 98.31 \\ c_{30} = g \left| \frac{AB(B/3 - m_2 l_1/4) + A(Cm_2 - Bm_2 l_1)/2}{(m_2/4 - A/3)(B^2 - AC) - m_2(B - Al_1)^2/4} \right| \\ = 11.44 \end{cases}$$

with $A = M + m_1 + m_2, B = m_1 l_1/2 + m_2 l_1$ and $C = m_1 l_1^2/3 + m_2 l_2^2$. The controller HRSMC parameters of the cart double inverted pendulum system are chosen as follows:

$$c_1 = 7.3170, c_2 = 3.8760, c_3 = 1.9560, a_1 = 0.8190, a_2 = 0.3170, k_3 = 3.5020, \eta_3 = 8.6910$$

The initial state vector is: $X_0 = [-0.1,0,0.1,0,0.1,0]^T$. The desired state vector is $X_d = [0,0,0,0,0,0]^T$ The HRFSMC controller parameters of the pendubot system are selected the same as the HRSMC controller parameters. However, HRFMC control has one more parameter selected are $k_1 = 0.01$ and$k_1 = 5$. Same as in section 5.1. To see the ability to remove chattering signals. HRFSMC controller with $k_1 = 0.01$ and $k_1 = 5$ is also compared with HRSMC controller.

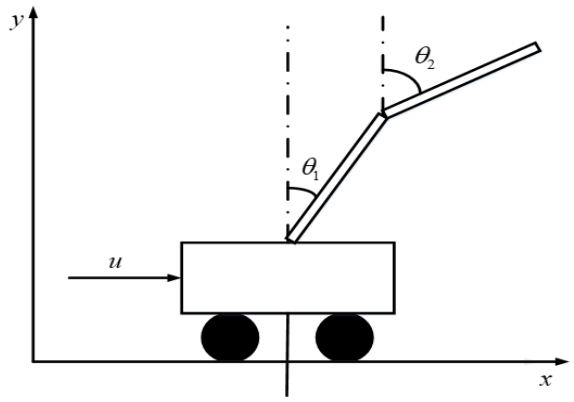

Figure 14. Architecture of the cart inverted pendulum system

Figures 15, 16, 17, 18, 19 compare the simulation results of two HRSMC and HRFSMC cart double inverted pendulum systems with $k_1 = 0.01$. It shows that angle of pendulum 1, pendulum 2, cart position of HRSMC and HRFSMC controllers converge to the equilibrium position for about 3.5 seconds. The Control force operating on the cart of HRFSMC control has oscillation, which is completely eliminated compared with the control force operating in the cart of HRSMC controller. The angles pendulum 1 and cart position of the HRFSMC controller has an oscillation which is completely disappeared compared with angles link 1 and cart position of the HRSMC controller. However, the HRSMC controller responds faster than the HRFSMC controller with $k_1 = 0.01$.

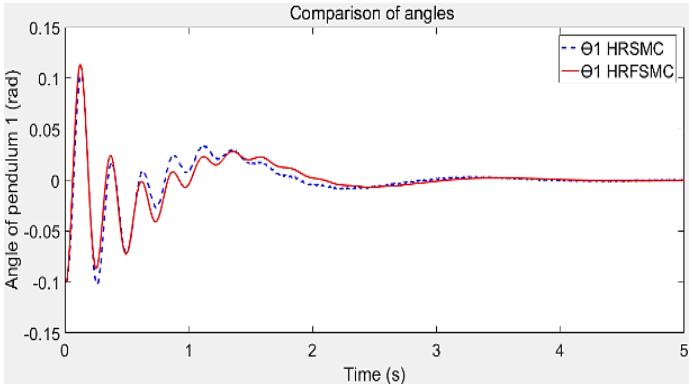

(a)

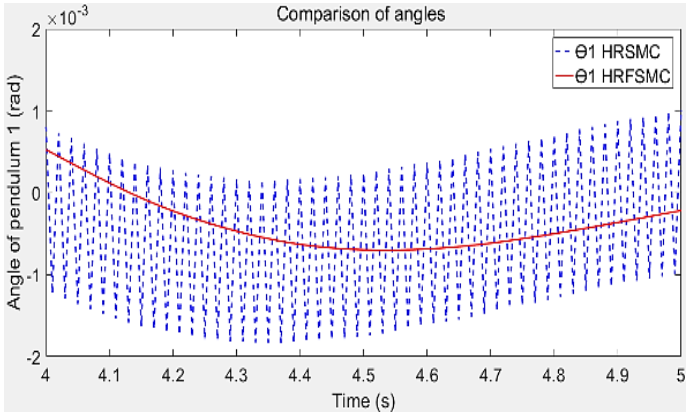

(b)

Figure 15. The pendulum angle 1 of the cart double inverted pendulum system when using the HRSMC control and the HRFSMC controller with $k_1 = 0.01$
(a) θ_1 in time series format; (b) Zoomed-in time frame of θ_1 (4–5s)

Figures 20, 21, 22, 23 compare simulation results of two controllers HRSMC and HRFSMC cart double inverted pendulum systems with $k_1 = 5$. It shows that angle of pendulum 1, pendulum 2, cart position of HRSMC and HRFSMC controllers converge to the equilibrium position for about 3.5 seconds. The control force operating on the cart of HRFSMC control has oscillation, which is smaller compared with the control force operating in the cart of HRSMC controller. The angles pendulum 1 and cart position of the HRFSMC controller has an oscillation which is smaller compared with angles link 1 and cart position of the HRSMC controller. However, the HRSMC controller responds equally to the HRFSMC controller with $k_1 = 5$.

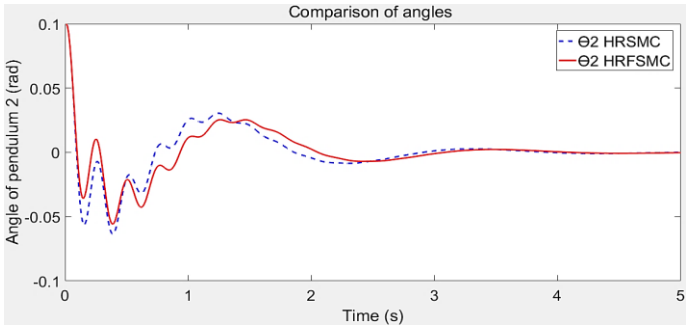

(a)

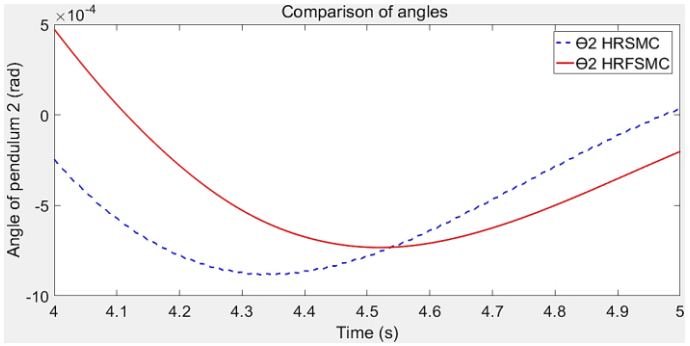

(b)

Figure 16. The pendulum angle 2 of the cart double inverted pendulum system using the HRSMC controller and the HRFSMC controller with $k_1 = 0.01$
(a) θ_1 in time series format; (b) Zoomed-in time frame of θ_1 (4 – 5 s).

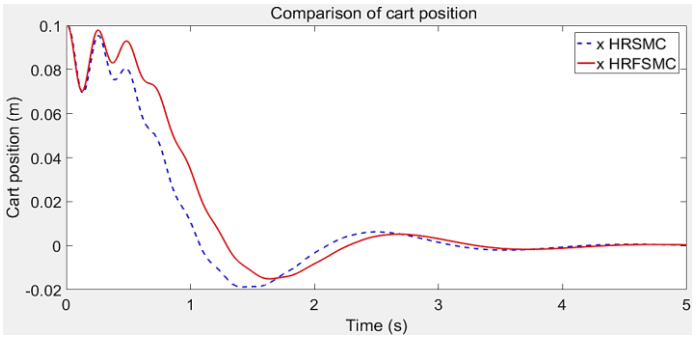

(a)

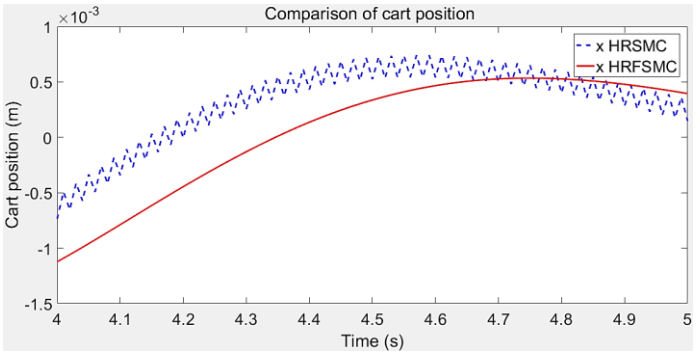

(b)

Figure 17. Cart position of the cart double inverted pendulum when using the HRSMC controller and the HRFSMC controller with $k_1 = 0.01$
(a) θ_1 in time series format; (b) Zoomed-in time frame of θ_1 (4 – 5 s)

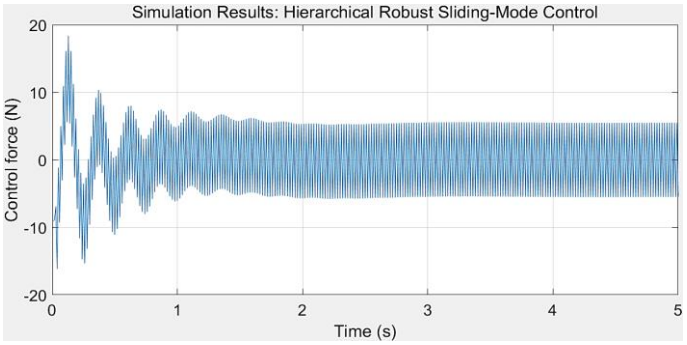

Figure 18. The action force on the cart of the cart double inverted pendulum system when using the HRSMC controller

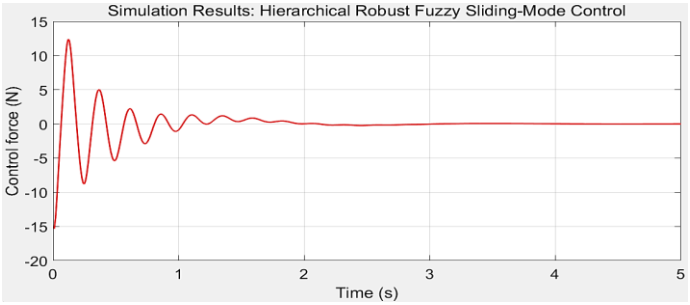

Figure 19. The action force on the cart of the cart double inverted pendulum system when using the HRFSMC controller with $k_1 = 0.01$

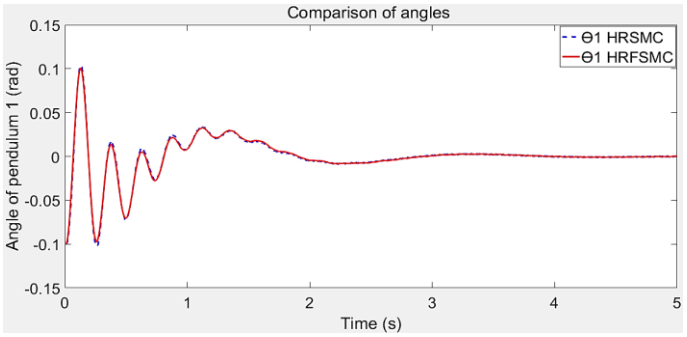

(a)

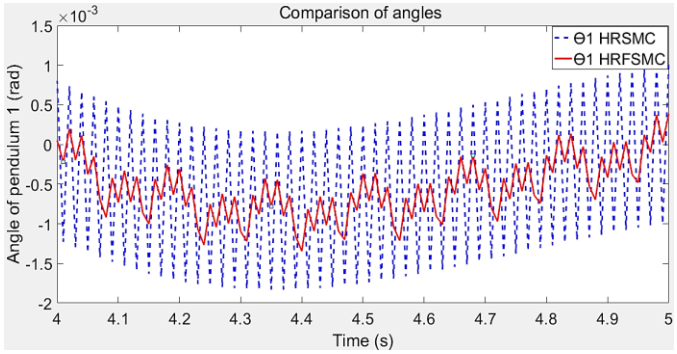

(b)

Figure 20. The pendulum angle 1 of the cart double inverted pendulum system when using the HRSMC control and the HRFSMC controller with $k_1 = 5$
(a) θ_1 in time series format; (b) Zoomed-in time frame of θ_1 (4 – 5 s)

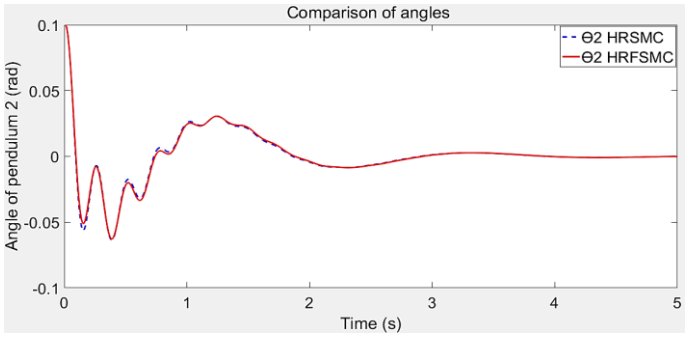

(a)

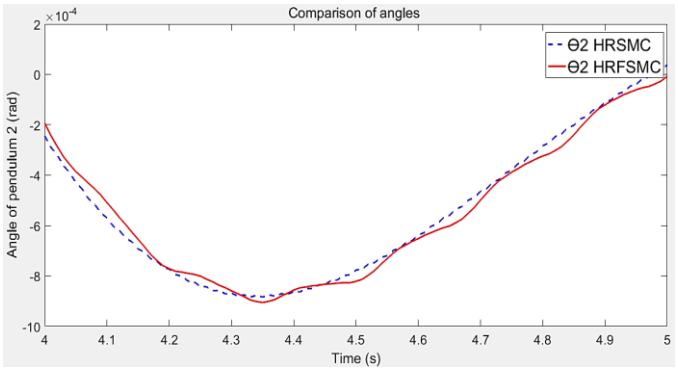

(b)

Figure 21. The pendulum angle 2 of the cart double inverted pendulum system using the HRSMC controller and the HRFSMC controller with $k_1 = 5$
(a) θ_1 in time series format; (b) Zoomed-in time frame of θ_1 (4 – 5 s).

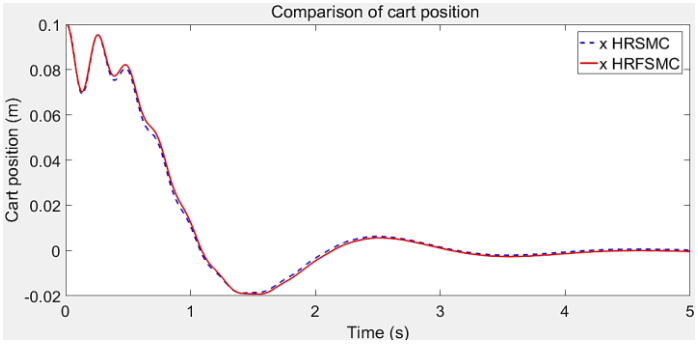

(a)

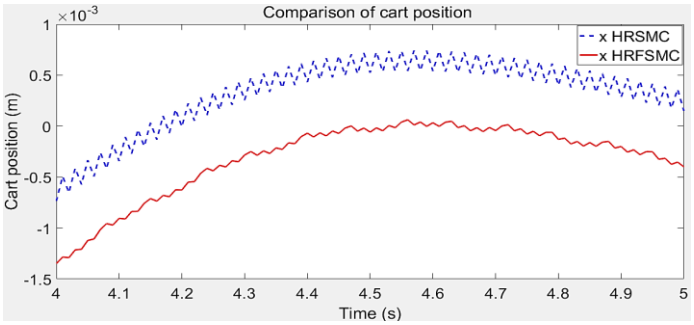

(b)

Figure 22. Cart position of the cart double inverted pendulum when using the HRSMC controller and the HRFSMC controller with $k_1 = 5$
(a) θ_1 in time series format; (b) Zoomed-in time frame of θ_1 (4 – 5 s)

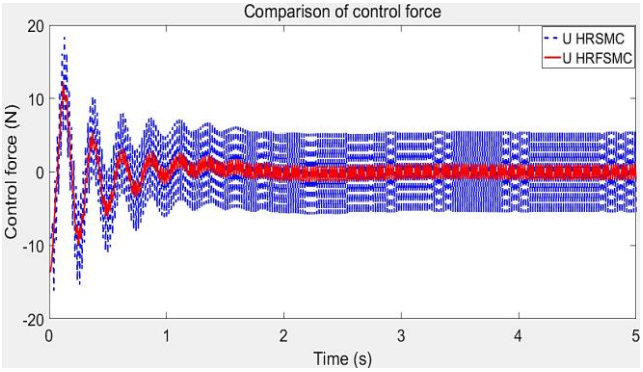

Figure 23. The action force on the cart of the cart double inverted pendulum system when using the HRSMC controller and the HRFSMC controller with

6. Conclusion

In this paper, a new compound HSMC and FLC control scheme has been proposed. It has been also successfully implemented to control the SIMO under-actuated systems for achieving high stability and robustness by combining the advantages of sliding mode control law and the FLC to completely removes the chattering signal. Based on Lyapunov stability theory and fuzzy control rules, the author has proven that the system is always stabilized and elimination of the chattering phenomenon throughout the work area. From the simulation results have shown that hierarchical robust fuzzy sliding mode controller in both systems pendubot and cart double inverted pendulum has completely eliminated chattering phenomena compared to the hierarchical robust sliding mode controller. The future research work, we can continue to research to put into experimental as well as be applied in practice.

References

[1] Xu R, Ozguner U. Sliding mode control of a class of underactuated systems. *Automatica.* 2008; 44(1): 233–241.
[2] Olfati-Saber R. Normal forms for underactuated mechanical systems with symmetry. *IEEE Transactions on Automatic Control*. 2002; 47(2): 305-308.
[3] Xin X, Kaneda M. Swing-Up Control for a 3-DOF Gymnastic Robot with Passive First Joint: Design and Analysis. *IEEE Transactions on Robotics*. 2007; 23(6): 1277-1285.
[4] Fierro R, Lewis F L, Lowe A. Hybrid control for a class of underactuated mechanical systems. *IEEE Transactions on Systems, Man, and Cybernetics-Part A: Systems and Humans*. 1999; 29(6): 649-654.
[5] Spong MW. The swing up control problem for the Acrobot. *IEEE Control Systems*. 1995; 15(1): 49-55.
[6] Fantoni I, Lozano R, Spong MW. Energy based control of the Pendubot. *IEEE Transactions on Automatic Control*. 2000; 45(4): 725-729.
[7] Xin X, Kaneda M. *New Analytical Results of the Energy Based Swinging up Control of the Acrobot.* Proceedings of the 43rd IEEE Conference on Decision and Control. 2004; 1: 704–709.
[8] Alleyne A. Physical insights on passivity-based TORA control designs. *IEEE Transactions on Control Systems Technology*. 1998; 6(3): 436-439.
[9] Zhang M, Tarn TJ. Hybrid control of the Pendubot. *IEEE/ASME Transactions on Mechatronics*. 2002; 7(1): 79-86.
[10] Yi J, Yubazaki N, Hirota K. A new fuzzy controller for stabilization of parallel-type double inverted pendulum system. *Fuzzy Sets and Systems*. 2002; 126(1): 105-119.
[11] Lai X, She JH, Ohyama Y, Cai Z. *Fuzzy control strategy for Acrobots combining model-free and model-based control.* IEEE Proceedings-Control Theory and Applications. 1999; 146(6): 505-510.
[12] Rubi J, Rubio A, Avello A. *Swing-up control problem for a self-erecting double inverted pendulum.* IEEE Proceedings-Control Theory and Applications. 2002; 149(2): 169-175.
[13] Ortega R, Spong MW, Gomez-Estern F, Blankenstein G. Stabilization of a class of underactuated mechanical systems via interconnection and damping assignment. *IEEE Transactions on Automatic Control*. 2002; 47(8): 1218-1233.
[14] Fang Y, Dixon WE, Dawson DM, Zergeroglu E. Nonlinear coupling control laws for an underactuated overhead crane system. *IEEE/ASME Transactions on Mechatronics*. 2003; 8(3): 418-423.

[15] Jung S, Wen JT. Nonlinear Model Predictive Control for the Swing-Up of a Rotary Inverted Pendulum. *ASME Journal of Dynamic Systems, Measurement and Control.* 2004; 126(1): 666-673.
[16] Baklouti F, Aloui S, Chaari A. Adaptive Fuzzy Sliding Mode Tracking Control of Uncertain Underactuated Nonlinear Systems: A Comparative Study. *Journal of Control Science and Engineering.* 2016; 2016:12.
[17] Hwang C, Chiang C, Yeh Y. Adaptive Fuzzy Hierarchical Sliding-Mode Control for the Trajectory Tracking of Uncertain Underactuated Nonlinear Dynamic Systems. *IEEE Transactions on Fuzzy Systems.* 2014; 22(2): 286-299.
[18] Hung L-C, Chung H-Y. Decoupled sliding-mode with fuzzy-neural network controller for nonlinear systems. *International Journal of Approximate Reasoning*. 2007; 46(1): 74-97.
[19] Shun-Feng S, Yao-Chu H, Cio-Ping T, Song-Shyong C, Yu-San L. Direct Adaptive Fuzzy Sliding Mode Control for Under-actuated Uncertain Systems. *International Journal of Fuzzy Logic and Intelligent Systems.* 2015; 15(4): 240-250.
[20] Slotine JJE, Li W. *Editors.* Applied Nonlinear Control. Englewood Cliffs: NJ: Prantice-Hall. 1991.
[21] Hung JY, Gao W, Hung JC. Variable structure control: a survey. *IEEE Transactions on Industrial Electronics*. 1993; 40(1): 2-22.
[22] Bartoszewicz A. Chattering attenuation in sliding mode control systems. *Control and Cybernetics*. 2000; 29(2): 585-594.
[23] Gao W, Hung JC. Variable structure control of nonlinear systems: a new approach. *IEEE Transactions on Industrial Electronics*. 1993; 40(1) 45-55.
[24] Wang W, Yi J, Zhao D, Liu D. Design of a stable sliding mode controller for a class of second-order underactuated systems. *IEEE Proceedings-Control Theory and Applications.* 2004; 151(6): 683–690.
[25] Qian DW, Yi JQ, Zhao DB. Hierarchical sliding mode control for a class of SIMO under-actuated systems. *Control and cybernetics*. 2008; 37(1): 159-175.
[26] Qian DW, Liu XJ, Yi JQ. Robust sliding mode control for a class of underactuated systems with mismatched uncertainties. *Proceedings of the Institution of Mechanical Engineers Part I Journal of Systems and Control Engineering*. 2008; 223(6): 785-795.
[27] Zakeri, Ehsan, et al. Robust sliding mode control of a mini unmanned underwater vehicle equipped with a new arrangement of water jet propulsions:Simulation and experimental study. *Applied Ocean Research.* 2016: 521-542.
[28] Li HX, Gatland HB, Green AW. Fuzzy variable structure control. *IEEE Transactions on Systems, Man, and Cybernetics, Part B (Cybernetics)*. 1997; 27(2): 306-312.
[29] Yu X, Man Z, Wu B. Design of fuzzy sliding-mode control systems. *Fuzzy Sets and Systems*. 1998; 95(3): 295-306.
[30] Chih-Min L, Yi-Jen M. Decoupling control by hierarchical fuzzy sliding-mode controller. *IEEE Transactions on Control Systems Technology*. 2005; 13(4): 593-598.
[31] Ji-Chang L, Ya-Hui K. Decoupled fuzzy sliding-mode control. *IEEE Transactions on Fuzzy Systems*. 1998; 6(3): 426-435.
[32] Qian D, Yi J. *Fuzzy aggregated hierarchical sliding mode control for underactuated systems*. 2010 IEEE International Conference on Mechatronics and Automation. 2010; 2010:196-201.
[33] Qian D, Yi J, Ma Y. *Fuzzy Incremental Hierarchical Sliding Mode Control for Underactuated Systems.* 2010 International Conference on Artificial Intelligence and Computational Intelligence. 2010; 2: 276-280.
[34] Zakeri E, Moezi SA, Eghtesad M. Optimal interval type-2 fuzzy fractional order super twisting algorithm: A second order sliding mode controller for fully-actuated and under-actuated nonlinear systems. *ISA transactions.* 2019; 85: 13-32.
[35] Zakeri E, Moezi SA, Eghtesad M. Tracking control of ball on sphere system using tuned fuzzy sliding mode controller based on artificial bee colony algorithm. *International Journal of Fuzzy Systems.* 2018; 20(1): 295-308.